Paper

An Investigation of the MIMO Space Time Block Code Based Selective Decode and Forward Relaying Network over η–μ Fading Channel Conditions

Ravi Shankar[1], V. V. Raghava Raman[2], Kantilal Pitamber Rane[3], Sarojini B. K.[4], and Rahul Neware[5]

[1] *Madanapalle Institute of Technology and Science, Madanapalle, India*
[2] *Aurora's Degree and PG College, Chikkadapally, Hyderabad, India*
[3] *Department of Electronics and Communication, K L University, Hyderabad, India*
[4] *Basaveshwar Engineering College, Bagalkot, Karnataka, India*
[5] *Høgskulen på Vestlandet, Bergen, Norway*

https://doi.org/10.26636/jtit.2022.150421

Abstract—In this paper, we examine the end-to-end average pairwise error probability (PEP) and output probability (OP) performance of the maximum ratio combining (MRC) based selective decode and forward (S-DF) system over an η–μ scattering environment considering additive white Gaussian noise (AWGN). The probability distribution function (PDF) and cumulative distribution function (CDF) expressions have been derived for the received signal-to-noise (SNR) ratio and the moment generating function (MGF) technique is used to derive the novel closed-form (CF) average PEP and OP expressions. The analytical results have been further simplified and are presented in terms of the Lauricella function for coherent complex modulation schemes. The asymptotic PEP expressions are also derived in terms of the Lauricella function, and a convex optimization (CO) framework has been developed for obtaining optimal power allocation (OPA) factors. Through simulations, it is also proven that, depending on the number of multi-path clusters and the modulation scheme used, the optimized power allocation system was essentially independent of the power relation scattered waves from the source node (SN) to the destination node (DN). The graphs show that asymptotic and accurate formulations are closely matched for moderate and high SNR regimes. PEP performance significantly improves with an increase in the value of η for a fixed value of μ. The analytical and simulation curves are in close agreement for medium-to-high SNR values.

Keywords—5G, MIMO, MRC, non-homogeneous fading channel, PEP, S-DF, SNR.

1. Introduction

With the explosive growth of cellular traffic, researchers are increasingly interested in improving performance of wireless networks in real-time propagation conditions. Therefore, they focus on the different systems, including massive multiple-input multiple-output (m-MIMO), device-to-device (D2D) communication, spatial modulation (SM) techniques, machine-to-machine (M2M) communication, non-orthogonal multiple access (NOMA) systems, and cooperative wireless communications over real-time propagation environments [1]–[4].

The use of multiple-input-multiple-output (MIMO) networks over multipath fading links can significantly increase spectral efficiency (SE) and quality of service (QoS). However, installation of multiple antennas is not possible in the case of some wireless devices. As a result, space time block code (STBC) introduces the cooperative diversity (virtual MIMO) approach to mitigate multipath fading and to increase diversity gains (DGs). In a $\frac{1}{2}$ transmit diversity system, Alamouti suggested in [4] that orthogonal space-time codes achieve DG levels that are comparable to those of MRC systems.

The increasing popularity of smartphones and tablets has recently accelerated the use of wireless local area networks (LAN). This means that a dense network of access points exists in apartments, buildings and public places, causing signal interference and increasing the time needed to transmit and receive data.

Cooperative communication is a very recent idea and stimulates the emergence of popular modern wireless communication systems, especially those characterized by high data rates or the fifth generation (5G) wireless communication systems. In 5G and beyond 5G wireless communication networks, cooperative communication schemes are seen as a practicable technique to expand network coverage while maintaining a high data rate [5]–[6]. Several developing applications have been implemented, including M2M networks, D2D networks, wireless sensor networks (WSNs) and vehicle-to-vehicle (V2V) 5G networks, to relay wireless networking. In a relaying network, the relay node (RN) receives the signal from the SN, manipulates it by

performing specific operations, e.g. some basic processing operations or complex and advanced signal processing operations that depend on the nature of the RN, and then it relays or forwards this signal to the DN.

In cooperative communication, the networks are divided into three popular categories: amplify-and-forward (AF), decode-and-forward (DF), and compress-and-forward (COF). The RNs decrypt incoming signals in DF systems and then forward the decoded signals back to the next RN, preventing noise spread. The AF protocol only amplifies the signal that is later forwarded to the next node. COF compresses, encodes and transmits received data to the next-hop device. However, the main drawbacks of the DF and AF approaches include noise amplification and erroneous signal propagation, respectively [7]–[8].

To fix the error propagation and noise amplification problem, the S-DF relaying protocol is considered in [9]–[11], under various fading channel conditions. In the case of S-DF relaying, the RN compares the threshold SNR with instantaneous SNR. If the threshold SNR is greater than instantaneous SNR, then the RN will remain idle. The authors examined a MIMO-STBC S-DF cooperative network under Rayleigh fading channel circumstances in [9]. The performance of the system is examined for OPA and equal power allocation (EPA) factors. The AF and S-DF protocols are compared, and the curves reveal that the S-DF protocol performs significantly better than the AF protocol.

The line of sight (LOS) scenario was not considered in the Rayleigh fading channel conditions. In the case of wireless channels, both fast fading and shadowing, sometimes also known as small-scale fading and large-scale fading, have been observed. Statistical distributions, such as Rayleigh, Nakagami-m, and Weibull, have been proposed in the literature to characterize small-scale variations in the fading channel envelope [10]–[11]. The average PEP analysis of the MIMO-STBC S-DF relaying network across the extended Nakagami-m fading channel conditions was explored in [12]. Both LOS and non-line of sight (NLOS) propagation scenarios were considered by the authors. In [13], the authors examined the S-DF relaying technique under keyhole fading channel conditions. Performance under keyhole Nakagami-m and Nakagami-m fading channel circumstances is compared. Symbol error rate (SER) performance under keyhole Nakagami-m fading channel conditions is worse than that under Nakagami-m fading channel circumstances, as shown by the simulation curves. However, whereas articles [10]–[13] looked at MIMO-S-DF performance under frequency flat time-invariant fading, in real-time propagation conditions, the channel becomes frequency selective, owing to multipath fading, and time selective due to movement between the communicating nodes.

The authors of paper [14] examined PEP and OP performance of the S-DF relaying protocol under time selective fading channel circumstances. In their study, the authors of [15]–[16] considered poor channel state information (CSI) and calculated the OPA factors. The authors of [15] examined OP and PEP performance of the MIMO STBC S-DF relaying network under time selective Nakagami-m fading channel circumstances, while accounting for poor CSI and node mobility. The results demonstrate that when node mobility increases, SER decreases considerably. The authors of [16] obtained the OP expression of the MIMO OSTBC and found the OPA factors under the time selective fading connections, while accounting for poor CSI. The PDF of the sum of i.i.d. gamma RVs and CDF is obtained and utilized for investigating performance of the cooperative communication system. To acquire the OPA factors, a mathematical framework is obtained. The results show that SN mobility has a higher influence than DN mobility on the average OP performance. As a result, cooperative systems are limited by an asymptotic error floor with a higher SNR value in other node mobility conditions. Simulation results show that the only ideal approach to distributing the power equally between the SN and RNs is possible when the SR fading link is stronger than the RD link.

However, none of those analyses considered non-homogeneous fading channel environments. Nonetheless, the documented performance and OPA experiments were conducted using Rician, Nakagami-m, and Nakagami-m fading channels. These fading channel models, as described in [9]–[15], are based on the concept of homogeneous scattering environments, which is not practical in most radio propagation scenarios, because the surfaces in the majority of spatial radio propagation environments are spatially correlated, as proven by previous research. The η–μ distribution, a generalized fading model used to give an especially precise fitting to genuine measurement data while also encompassing the well-known Rayleigh, Nakagami-m, and Hoyt distributions as specific instances, was proposed to solve this issue in [17]. The distribution was proven to have properly accommodated small-scale variations in the NLOS communication situations, where the two parameters designated η and μ are defined and valid for two distinct forms which correspond to two physical models, as described in paper [17]. In addition, work [18] gives the PDF of the immediate SNR.

2. Related Work

In 5G networks, stochastic modeling and characterization of the wireless fading channel have a significant impact on bit error rate (BER) and OP performance. So, precise channel modeling is necessary for identifying 5G communication protocols and techniques that are efficient and cost-effective. However, the fading distributions described in the literature fail to take into consideration non-linearity of the medium.

Under non-homogeneous circumstances, such as α–μ, κ–μ, and η–μ, an exact OP calculation for diversity receivers was provided in [17]. Yacoub proposed η–μ fading in [17] as a generalized distribution to describe diverse fading situations. The η–μ distribution may also be used

to represent non-LOS situations. For the study of wireless communication networks, several researchers utilize the η–μ fading distribution. η–μ distribution also simulates generalized fading, such as Nakagami-m fading.

The MRC approach was chosen as one of the diversity receivers in [18], and a detailed performance study of the L-branch system over η–μ fading channels considering imperfect CSI was presented. The authors have investigated the OP and SER performance under $\alpha-\mu$ fading channel scenarios, considering 4-quadrature amplitude modulation (QAM) techniques. For mmWave fluctuating two-ray fading links, an SER investigation was performed in [19]. In [20], the authors derived the CF expression of the average SER and BER for M-ary cross QAM symbols with MRC diversity reception over i.i.d. η–μ fading links. Rectangular and cross QAM methods were also investigated in a similar manner in [21]. In [22], the net throughput for relaying users in a NOMA network over κ–μ shadowed fading channels was analytically evaluated.

In [23], the authors investigated OP and SER for κ–μ shadowing distribution, in an interference-limited scenario. In [24], the authors studied spatial modulation techniques over α–μ, κ–μ, and η–μ fading channel models. Using non-homogeneous channel distributions, the research conducted in [25]–[29] examined physical layer security and secrecy capacities for various system models. In [25], the authors examined secrecy capacity over κ–μ fading channels. In [26], the authors examine the secrecy capacity performance over κ–μ fading connections for MIMO networks [26]. To significantly improve on the results of the analysis performed in [26], a complete physical layer security study for MIMO networks was given in article [27], under the η–μ and λ–μ fading scenarios.

As an alternative, in [28], the authors investigated secrecy capacity for wireless communication networks under α–μ fading conditions. As it was the case in [25]–[29], they also examined physical layer security for a α–κ–μ and α–η–μ fading scenarios, with SISO fading links. Three parameters of the fading models were examined as well, namely α, η, μ or α, η, μ.

In papers [30]–[33], the authors examined AF, best relay selection (BRS) DF, and cognitive AF (CAF) relaying networks. In [30], the authors verified SER performance of dual hop (DH) CAF relaying networks over η–μ fading channels. Under mixed κ–μ and η–μ circumstances, in [31], the authors investigated α–μ fading channels. Mixed-fading links were utilized to evaluate performance of the BRS approach for D2D wireless networks [32].

In the literature, only the well-known AWGN noise was taken into account when evaluating the performance of different system models across non-homogeneous fading channels. The α–η–μ distribution is a fading distribution used in N-LOS communications to characterize small-scale variations in a faded signal. In the α–η–μ distribution, the fading signal is composed of numerous multipath clusters traveling across a non-homogeneous medium. Nonlinearity of the propagation medium and the number of clusters are represented by the exponents α and μ, respectively. The α–μ distribution may be used to produce Rayleigh, Nakagami-m, and Weibull fading channel distributions. To assess performance of the system through multiple fading models, the α–μ model can be employed. Paper [34] indicates that several common decaying distributions are generated in a precise manner by α–μ, α–μ, and μ values, including η–μ, α–μ, λ–μ, Nakagami-m, exponential, Weibull, one-sided Gaussian, Hoyt, and Rayleigh. The α–η–μ distribution may also be used to approximate the Rice and lognormal distributions. The authors of [34] looked at BER performance of the DF relaying network under α–μ fading channel conditions. The end-to-end SNR's PDF, CDF, and MGF were calculated in this work. CF expressions for the system's average OP, net throughput, and average BER were calculated as well. The resulting expressions may be used to compare the performance of multi-hop relaying networks with other well-known fading channel models, by simply inserting the relevant values for the α and μ parameters. In [35], the authors looked at BER performance of a DH AF beamforming network with multiple antennas, only at the DN and SNs and with both hops subjected to κ–μ fading channel circumstances.

The κ–μ fading channel model is of the generalized variety and may properly represent realistic fast fading in LOS scenarios. It also includes specific cases for Rayleigh, Rician, and Nakagami-m scenarios. In article [36], the authors derived the CF expressions of the OP, average BER, and net throughput for a MIMO STBC S-DF relaying network over κ–μ fading channel conditions. They analyzed those fading links that are subjected to i.i.d. κ–μ fading conditions. According to simulation results, the stronger LOS component increases BER performance. It has been demonstrated that the in the case of LOS scenarios, MIMO STBC S-DF relaying systems can function effectively, and BER performance improves significantly. Through MC simulations, it was determined that theoretical findings closely matched the actual results, thus validating the derivations produced. In [37], the authors investigated 5G heterogeneous cellular systems operating over κ–μ shadowed fading channels. Furthermore, asymptotic outcomes for BER, net throughput and OP were obtained in simpler forms of fundamental functions, making the system's behavior and the influence of channel parameters understandable. These theoretical outcomes are general and they may be used to simulate a variety of asymmetric and symmetric fading scenarios, including Nakagami-m, Rayleigh, Rician, and mixed κ–μ fading connections. In [38], the authors researched a DH AF cooperative communications system, where RD and SR fading links are subject to mixed η–μ and κ–μ fading channel conditions. The RN is assumed to be fixed gain and perfect CSI conditions are considered. The modeling of realistic DH transmissions is enabled by the use of such mixed η–μ and κ–μ fading channels. It is possible to obtain accurate theoretical expressions for OP and for average BER of various complex modulation techniques, in the form of fast converging infinite series. In [39], the

authors derived a mathematical framework for investigating BER and channel capacity of the relaying network over an inverse gamma shadowing fading channel. Firstly, the paper examined the advantages of inverse gamma over gamma fading and log-normal fading models. Novel PDF and CDF expressions were derived and the analytical results for BER and channel capacity of selection combining diversity are presented.

In [40], the authors investigated channel capacity over the inverse gamma and η–μ composite fading channels. To achieve that aim, precise theoretical expressions for net throughput were derived, along with simple tight-bound representations. Additionally, simple approximation formulas for the high SNR regime were presented. Next, net throughput was examined under various shadowing, multipath fading, and delay constraints scenarios. The simulation results show that as the multipath fading and shadowing parameters decrease, or the delay restriction rises, the attainable SE decreases significantly. The authors of [41] derived the CDF of the sum of the α–μ, κ–μ, and η–μ RVs in the context of rare event Monte Carlo simulations. A less complex and extremely efficient sampling scheme was proposed to obtain higher diversity gains. The main consequence of this approach is the relative BER of the suggested estimators that are constrained by certain limits. The authors estimated the OP of multibranch MRC and equal gain diversity receivers over α–μ, κ–μ, and η–μ faded links of the kind articles [36]–[41] with great accuracy.

In [42], the authors derived PDF of the instantaneous SNR at the receiver side and investigated BER and asymptotic BER performance of uplink SIMO networks with AWGN noise over the non-homogeneous fading conditions, such as η–μ, λ–μ, and κ–μ. The OP and BER performances is shown for several fading parameter settings, receiver antenna counts, modulation methods, and noise type combinations to illustrate these points. These simulations are then used to verify correctness of the analytical frameworks suggested for the systems concerned.

In [43], the authors investigated a DF-based MIMO network over the κ–μ, η–μ, and mixed κ–μ and η–μ fading scenarios. After applying the MGF scheme, they derived novel expressions of BER, considering the M-ary PSK modulation symbols. Additionally, for high SNR, asymptotic BER expressions were examined to obtain OPA factors at the SN and RNs. The DO expression is derived for various types of non-homogeneous fading channel distributions. As far as OPAs are concerned, the impact of the SD distance on the performance of a fixed-relay network was analyzed.

In earlier studies concerned with the performance of different system models over non-homogeneous fading channels, including those cited above, the well-known AWGN type of channel was investigated only. Many outdoor, indoor, and underwater applications make the AWGN distribution problematic. Also, it is not taken advantage of in ultra-wideband wireless networks to reduce impulsive noise and multiuser interference [44]–[45]. However, as far as we know, no work has been devoted to PEP performance of the MIMO STBC network over η–μ.

Against this background we propose, in this paper, some novel expressions of PEP for the MIMO STBC network by considering non-homogeneous channels – not only to eliminate the disadvantages of the AWGN model but also to present PEP performance of the MIMO STBC network with AWGN over η–μ fading channels.

The main contributions of our paper include the following:

- performance of the MIMO STBC network over η–μ fading channels is theoretically analyzed in terms of PEP;
- approximate CF average PEP is derived, using MGF, are derived for the η–μ fading conditions under consideration;
- asymptotic PEP expressions of MIMO STBC networks over non-homogeneous channels are analyzed and compared with approximate results;
- CO framework is developed for finding DO and for identifying optimal source-relay power allocation factors;
- in order to validate the theoretical analysis, extensive computer simulations are performed. Simulations fully agree with our numerical results obtained in the course of the proposed analysis.

The mathematical expressions discussed in this work are denoted by the following notations. The Lauricella function and the Euclidean norm are represented by $F_A^{(1)}$ and $||X||_F$, respectively. The conjugate transpose, absolute value, and trace of matrix X are represented by $X^H, |X|$, and trace (X), respectively. $\mathrm{E}\{.\}$ is the expectation operator, and $J_0\{.\}$ denotes the 1st kind and 0th order Bessel function. The gamma function and the lower incomplete gamma function are represented by $\Gamma(.)$ and $\gamma(,)$, respectively. $P(\mathrm{X} > \mathrm{u})$ denotes the chance that a given value of a standard normal random variable X is larger than a specified value u.

The rest of the paper is organized as follows. The model of a MIMO-STBC-based S-DF relaying system over η–μ fading channel conditions is presented in Section 2. Section 3 derives the per-block average PEP, OP, asymptotic error floor, and asymptotic PEP expressions for the MIMO-STBC over η–μ fading channel conditions. Section 4 presents simulation outcomes, while Section 5 concludes the paper.

3. System Model

Consider a MIMO-STBC S-DF relaying network and let $\mathrm{S} \in \mathrm{C}^{K\times\varphi}$ denote the Alamouti STBC code-word matrix transmitted from the SN. The MIMO-STBC-based S-DF network is equipped with K number of antennas over the φ time slots. The SN transmits the $\mathrm{S} \in \mathrm{C}^{K\times\varphi}$ codeword to the DN and RN simultaneously. The codewords received at

the DN and RN are represented as $B_{SD} \in C^{K_D \times \varphi}$ and $B_{SR} \in C^{K \times \varphi}$, respectively. Figure 1 is a schematic representation of the S-DF relaying protocol over η–μ fading channel conditions.

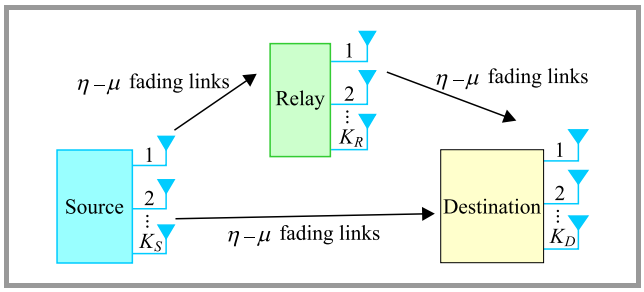

Fig. 1. Schematic representation of the S-DF relaying protocol over η–μ fading channel conditions.

Since the Alamouti STBC codeword is considered at both the RN and SN, the corresponding data rate will be the same and, hence, we are considering $K_S = K_R = K$. The received $\mathrm{B}_{SD} \in \mathrm{C}^{K_D \times \varphi}$ and $\mathrm{B}_{SR} \in \mathrm{C}^{K \times \varphi}$ codewords can be expressed as [18]–[20]:

$$\mathrm{B}_{SD} = \sqrt{\frac{\Phi_0}{K}}\mathrm{Z}_{SD}\mathrm{S} + \Pi_{SD} \ , \tag{1}$$

$$\mathrm{B}_{SR} = \sqrt{\frac{\Phi_0}{K}}\mathrm{Z}_{SR}\mathrm{S} + \Pi_{SR} \ , \tag{2}$$

where $\mathrm{Z}_{SD} \in \mathrm{C}^{K_D \times K}$ and $\mathrm{Z}_{SD} \in \mathrm{C}^{K_D \times K}$ represent the fading channel matrices between the SD and SR fading links, respectively. Φ_0 represents the power transmitted from the SN. Matrices Π_{SD} and Π_{SR} consist of AWGN noise samples at the DN and RN, respectively. Each noise sample is modeled as $\mathrm{CN}(0, N_0)$, i.e. complex circularly symmetric AWGN with zero mean and K_0 variance. These channel matrices consist of the η–μ faded channel coefficients with PDF [20]–[22]:

$$\mathrm{pd}f_{\kappa_i}(\kappa_i) = \frac{2\sqrt{\pi}\mu_i^{\mu_i+\frac{1}{2}} z_i^{\mu_i} \kappa_i^{\mu_i-\frac{1}{2}}}{\Gamma(\mu_i) Z_i^{\mu_i-\frac{1}{2}} \bar{\kappa}_i^{\mu_i+\frac{1}{2}}} \mathrm{e}^{\frac{-2\mu_i z_i \kappa_i}{\bar{\kappa}_i}} \times I_{\mu_i-\frac{1}{2}}\left(\frac{2\mu_i Z_i \kappa_i}{\bar{\kappa}_i}\right) \in \{SD, SR\} \ , \tag{3}$$

where κ_i is the instantaneous SNR and $\bar{\kappa}_i = \frac{\Phi_0 \upsilon_{jn}^2 \delta_i^2}{4KK_0}$ denotes the average SNR. The average channel gain is represented as δ_i^2, Z_i and z_i are the functions of fading parameters η_i defined in [22] and μ_i is the fading parameter. υ_{jn} denotes the singular values (SVs) obtained after performing the singular value decomposition (SVD) of the codeword difference matrix $\mathrm{S}_0 - \mathrm{S}_j$ and $I_x(.)$ is the modified Bessel function of the first kind and order x. At the RN, S-DF protocol is employed and the RN will forward the signal received from the SN when the received instantaneous SNR will be greater than the threshold SNR. The codeword forwarded from the RN to the DN, denoted by $\mathrm{B}_{RD} \in \mathrm{C}^{K_D \times \varphi}$ is expressed as:

$$\mathrm{B}_{RD} = \sqrt{\frac{\Phi_1}{K}}\mathrm{Z}_{RD}\mathrm{S} + \Pi_{RD}, \tag{4}$$

where Φ_1 represents the power transmitted at the RN. The MIMO channel matrix Z_{RD} consists of $\eta - \mu$ distributed fading channel coefficients with PDF as:

$$\mathrm{pd}f_{\kappa_{RD}}(\kappa_{RD}) = \frac{2\sqrt{\pi}\mu_{RD}^{\mu_{RD}+\frac{1}{2}} z_{RD}^{\mu_{RD}} \kappa_{RD}^{\mu_{RD}-\frac{1}{2}}}{\Gamma(\mu_{RD}) Z_{RD}^{\mu_{RD}-\frac{1}{2}} \bar{\kappa}_{RD}^{\mu_{RD}+\frac{1}{2}}} \mathrm{e}^{\frac{-2\mu_{RD} z_{RD} \kappa_{RD}}{\bar{\kappa}_{RD}}} \times I_{\mu_{RD}-\frac{1}{2}}\frac{2\mu_{RD} Z_{RD} \kappa_{RD}}{\bar{\kappa}_{RD}} \ , \tag{5}$$

where Z_{RD} and z_{RD} are the functions of fading parameters η_{RD} defined in [22] and $\mu_{RD} > 0$ is the fading parameter. Π_{RD} matrices at the destination corresponding to the transmission from RN, consist of noise samples with zero mean and variance equal to $\frac{K_0}{2}$ (per dimension).

4. PEP Analysis of MIMO-STBC S-DF Relaying Protocol

4.1. PEP Analysis

We commence our analysis by deriving the average PEP expression for the MIMO-STBC (single relay system), as shown in Fig. 1. Let $C = \{\mathrm{S}_j\}$ represent the codeword set, where codeword matrix $\mathrm{S}_j \in \mathrm{C}^{K \times \varphi}$ and $1 \leq j \leq |C|$, where $|C|$, represents the number of elements of the codeword set C. The end-to-end PEP of the erroneous event corresponding to $\mathrm{S}_0 \in \mathrm{C}^{K \times \varphi}$ being confused for the codeword $\mathrm{S}_j \in \mathrm{C}^{K \times \varphi}$ at the RN, where $j \neq 0$, conditioned on the channel matrix Z_{SR}, is expressed as [23]:

$$P_{S \to R}\left(\mathrm{S}_0 \to \frac{\mathrm{S}_j}{\mathrm{Z}_{SR}}\right) = Q\left(\sqrt{\kappa_{SR}}\right) \ , \tag{6}$$

where $\kappa_{SR} = \frac{\Phi_0 \left\| \mathrm{Z}_{SR}(\mathrm{S}_0 - \mathrm{S}_j) \right\|_F^2}{2KK_0}$ denotes the instantaneous SNR for SR fading link, $\mathrm{S}_0 \to \mathrm{S}_j$ represents the erroneous event and $P_{S \to R}$ represents the error probability for the SN to RN transmission. Let the SVD of the codeword difference matrix $\mathrm{S}_0 - \mathrm{S}_j$ be represented as $\mathrm{S}_0 - \mathrm{S}_j = U_j \Lambda_j V_j^H$, where $U_j \in \mathrm{C}^{K \times K} = I_K$, and the diagonal matrix $\Lambda_j \in \mathrm{R}^{K \times K}$ be represented as [23]:

$$\Lambda_j = \begin{bmatrix} \upsilon_{j,1} & 0 & 0 & \dots & 0 \\ 0 & \upsilon_{j,2} & 0 & \dots & 0 \\ 0 & 0 & \upsilon_{j,3} & \dots & 0 \\ 0 & 0 & 0 & \dots & \upsilon_{j,K} \end{bmatrix}_{K \times K} \ . \tag{7}$$

It contains the positive SVs $\upsilon_{j,1}, \upsilon_{j,2}, \dots, \upsilon_{j,K}$ of the codeword difference matrix. The $\mathrm{V}_j^H \in C^{\varphi \times K}$ matrix contains orthogonal row vectors which form a basis for the row space of the difference matrix $\mathrm{S}_0 - \mathrm{S}_j$, and satisfying the property $\mathrm{V}_j \mathrm{V}_j^H = I_K$. The Frobenius norm $\left\| \mathrm{Z}_{SR}(\mathrm{S}_0 - \mathrm{S}_j) \right\|_F^2$ can therefore be simplified as [23]:

Using $\mathrm{S}_0 - \mathrm{S}_j = U_j \Lambda_j V_j^H$ in the above expression, the $\left\|\mathrm{Z}_{SR}(\mathrm{S}_0 - \mathrm{S}_j)\right\|_F^2$ can be expressed as:

$$\left\|\mathrm{Z}_{SR}(\mathrm{S}_0 - \mathrm{S}_j)\right\|_F^2 = \mathrm{Tr}\left\{\mathrm{Z}_{SR} U_j \Lambda_j V_j^H V_j \Lambda_j U_j^H \mathrm{Z}_{SR}^H\right\} = \mathrm{Tr}\left\{\mathrm{Z}_{SR} U_j \Lambda^2{}_j U_j^H \mathrm{Z}_{SR}^H\right\} = \mathrm{Tr}\left\{\Lambda_j^2 \tilde{\mathrm{Z}}_{SR} \tilde{\mathrm{Z}}_{SR}^H\right\} = \sum_{n=1}^{K} \upsilon_{jn}^2 \sum_{\tilde{n}=1}^{K} |\tilde{z}_{\tilde{n},n}|^2 \ , \quad (8)$$

where coefficient $\tilde{z}_{\tilde{n},n}$ is the $(\tilde{n}, n)$ entry of matrix $\tilde{\mathrm{Z}}_{SR} = \mathrm{Z}_{SR} U_j$ for $1 \leq \tilde{n},\ n \leq K$. Therefore, the above expression for the PEP conditioned on the Z_{SR} can be simplified by substituting this expression for $\left\|\mathrm{Z}_{SR}(\mathrm{S}_0 - \mathrm{S}_j)\right\|_F^2$ as [20]:

$$P_{S\to R}\left(\frac{\mathrm{S}_0 \mathrm{S}_j}{\tilde{\mathrm{Z}}_{SR}}\right) = Q\left(\sqrt{\frac{\Phi_0 \sum_{n=1}^{K} \nu_{jn}^2 \sum_{\tilde{n}=1}^{K} |\tilde{z}_{\tilde{n},n}|^2}{2KK_0}}\right) . \quad (9)$$

Further, it can be readily seen that the gain $|\tilde{z}_{\tilde{n},n}|^2$ is η–μ distributed. The MGF is expressed as [20]–[22]:

$$MGF_{\kappa_{\eta-\mu}}\left(\frac{g_{PSK}}{\sin^2(\theta)}\right) = \left(\frac{4\mu_{SR}^2 z_{SR}}{\left[2(z_{SR}-\mathrm{Z}_{SR})\mu_{SR} + \frac{g_{PSK}\bar{\kappa}_{SR}}{\sin^2(\theta)}\right]\left[2(z_{SR}+\mathrm{Z}_{SR})\mu_{SR} + \frac{g_{PSK}\bar{\kappa}_{SR}}{\sin^2(\theta)}\right]}\right)^{\mu_{SR}} , \quad (10)$$

where $\bar{\kappa}_{SR} = \frac{\Phi_0 \upsilon_{jn}^2 \delta_{SR}^2}{4KK_0}$ denotes the average SNR and $g_{PSK} = \sin^2(\frac{\pi}{M})$.

$$P_{S\to R}(\mathrm{S}_0 \to \mathrm{S}_j) = \frac{1}{\pi}\int_0^{\frac{\pi}{2}} \frac{\left(4\mu_{SR}^2 z_{SR}\right)^{\mu_{SR}}\left[2(z_{SR}-\mathrm{Z}_{SR})\mu_{SR} + \frac{g_{PSK}\bar{\kappa}_{SR}}{\sin^2(\theta)}\right]^{-\mu_{SR}}}{\left[2(z_{SR}+\mathrm{Z}_{SR})\mu_{SR} + \frac{g_{PSK}\bar{\kappa}_{SR}}{\sin^2(\theta)}\right]^{\mu_{SR}}} \mathrm{d}\theta \ , \quad (11)$$

The solution of $P_{S\to R}(\mathrm{S}_0 \to \mathrm{S}_j)$ is as follows. Let $\cos^2(\theta) = t$. This will yield:

$$\sin^2(\theta) = 1 - \cos^2(\theta) = 1 - t \ , \quad (12)$$

$$-2\cos(\theta)\sin(\theta)\mathrm{d}\theta = \mathrm{d}t \ , \quad (13)$$

The upper and lower limits of the integral will become 0 and 1, respectively. Also, $\mathrm{d}\theta$ will become:

$$\mathrm{d}\theta = \frac{-\mathrm{d}t}{2\sqrt{t}\sqrt{1-t}} . \quad (14)$$

Then $P_{S\to R}(\mathrm{S}_0 \to \mathrm{S}_j)$ can be expressed as:

$$P_{S\to R}(\mathrm{S}_0 \to \mathrm{S}_j) = \frac{2^{2\mu_{SR}}\left(4\mu_{SR}^2 z_{SR}\right)^{\mu_{SR}}}{2\pi\left[4(z_{SR}-\mathrm{Z}_{SR})\mu_{SR} + 2\bar{\kappa}_{SR}\right]^{\mu_{SR}}\left[4(z_{SR}+\mathrm{Z}_{SR})\mu_{SR} + 2\bar{\kappa}_{SR}\right]^{\mu_{SR}}} \times \int_0^1 \frac{t^{-\frac{1}{2}}(1-t)^{2\mu_{SR}-\frac{1}{2}}\mathrm{d}t}{\left[1 - \frac{4(z_{SR}-\mathrm{Z}_{SR})\mu_{SR}t}{4(z_{SR}-\mathrm{Z}_{SR})+2\bar{\kappa}_{SR}}\right]^{\mu_{SR}}\left[1 - \frac{4(z_{SR}+\mathrm{Z}_{SR})\mu_{SR}t}{4(z_{SR}-\mathrm{Z}_{SR})+2\bar{\kappa}_{SR}}\right]^{\mu_{SR}}} , \quad (15)$$

$$P_{S\to R}(\mathrm{S}_0 \to \mathrm{S}_j) = M_{\kappa_{SR}}(1)\int_0^1 \frac{t^{-\frac{1}{2}}(1-t)^{2\mu_{SR}-\frac{1}{2}}\mathrm{d}t}{\left[1 - \frac{4(z_{SR}-\mathrm{Z}_{SR})\mu_{SR}t}{4(z_{SR}-\mathrm{Z}_{SR})+2\bar{\kappa}_{SR}}\right]^{\mu_{SR}}\left[1 - \frac{4(z_{SR}+\mathrm{Z}_{SR})\mu_{SR}t}{4(z_{SR}-\mathrm{Z}_{SR})+2\bar{\kappa}_{SR}}\right]^{\mu_{SR}}} , \quad (16)$$

where

$$MGF_{\kappa_{SR}}(s) = \frac{\left(4\mu_{SR}^2 z_{SR}\right)^{\mu_{SR}}}{\left[2(z_{SR}-\mathrm{Z}_{SR})\mu_{SR} + s\bar{\kappa}_{SR}\right]^{\mu_{SR}}\left[2(z_{SR}+\mathrm{Z}_{SR})\mu_{SR} + s\bar{\kappa}_{SR}\right]^{\mu_{SR}}} . \quad (17)$$

The Appell hypergeometric function of two variables is expressed as [29]:

$$F_A^{(1)}\left(\tau; \vartheta, \vartheta'; \Xi; \dagger; \diamondsuit\right) = \frac{\Gamma(\Xi)}{\Gamma(\tau)\Gamma(\Xi-\tau)}\int_0^1 t^{\tau-1-\frac{1}{2}}(1-t)^{\Xi-\tau-1}(1-tx)^{-\vartheta}(1-ty)^{-\vartheta'}\mathrm{d}t . \quad (18)$$

Comparing Eq. (17) with Eq. (18) we get:

$$\tau = \frac{1}{2}, \quad \vartheta = 1, \quad \vartheta' = 1, \quad \Xi = 2\mu_{SR} + 1 \ , \quad (19)$$

$$\dagger = \frac{4(z_{SR}-\mathrm{Z}_{SR})\mu_{SR}}{4(z_{SR}+\mathrm{Z}_{SR})\mu_{SR} + 2\bar{\kappa}_{SR}} , \quad (20)$$

and

$$\diamondsuit = \frac{4(z_{SR}+\mathrm{Z}_{SR})\mu_{SR}}{4(z_{SR}+\mathrm{Z}_{SR})\mu_{SR} + 2\bar{\kappa}_{SR}} . \quad (21)$$

Therefore, $P_{S\to R}(\mathrm{S}_0 \to \mathrm{S}_j)$ can be expressed as:

$$P_{S\to R}(\mathrm{S}_0 \to \mathrm{S}_j) = \frac{1}{2\pi} MGF_{\kappa_{SR}}(1)\frac{\Gamma(\frac{1}{2})\Gamma(2\mu_{SR}+\frac{1}{2})}{\Gamma(2\mu_{SR}+1)} \times F_A^{(1)}\left(\frac{1}{2};\ 1, 2\mu_{SR}+1;\ \frac{4(z_{SR}-\mathrm{Z}_{SR})\mu_{SR}}{4(z_{SR}-\mathrm{Z}_{SR})\mu_{SR} + 2\bar{\kappa}_{SR}};\ \frac{4(z_{SR}+\mathrm{Z}_{SR})\mu_{SR}}{4(z_{SR}+\mathrm{Z}_{SR})\mu_{SR} + 2\bar{\kappa}_{SR}}\right) . \quad (22)$$

The overall possible space-time block-code codeword's $\mathrm{S}_j \in C$, the upper bound of $P_{S\to R}(\mathrm{S}_0 \to \mathrm{S}_j)$ is expressed as:

$$\bar{P}_{S\to R} \leq \sum_{\mathrm{S}\in C, \mathrm{S}_j \neq X_0} P_{S\to R}(\mathrm{S}_0 \to \mathrm{S}_i) . \quad (23)$$

With a similar procedure applied, the average PEP for the SD fading link is expressed as:

$$\bar{P}_{S\to D} = \frac{1}{2\pi} MGF_{\kappa_{SD}}(1)\frac{\Gamma(\frac{1}{2})\Gamma(2\mu_{SD}+\frac{1}{2})}{\Gamma(2\mu_{SD}+1)} \times F_A^{(1)}\left(\frac{1}{2};\ 1, 2\mu_{SD}+1;\ \frac{4(z_{SD}-\mathrm{Z}_{SD})\mu_{SD}}{4(z_{SD}-\mathrm{Z}_{SD})\mu_{SD} + 2\bar{\kappa}_{SD}};\ \frac{4(z_{SD}+\mathrm{Z}_{SD})\mu_{SD}}{4(z_{SD}+\mathrm{Z}_{SD})\mu_{SD} + 2\bar{\kappa}_{SD}}\right) . \quad (24)$$

Let $\tilde{z}_{\tilde{l}n}^{(SD)}, \tilde{z}_{ln}^{(RD)}$ represent the η–μ fading channel coefficients corresponding to the effective SD and RD matrices $\tilde{\mathrm{Z}}_{SD} = \mathrm{Z}_{SD}U_i$ and $\tilde{\mathrm{Z}}_{RD} = \mathrm{Z}_{RD}U_i$, respectively. For erroneous event $\mathrm{S}_0 \to \mathrm{S}_i$ at the DN, when the RN decodes all the data symbols transmitted by the SN during the first signaling phase successfully, conditioned on the SD and RD channel matrices $\tilde{\mathrm{Z}}_{SD}, \tilde{\mathrm{Z}}_{RD}$, P_S is expressed below:

$$P_{S\to D,R\to D}(\mathrm{S}_0 \to \frac{\mathrm{S_i}}{\tilde{\mathrm{Z}}_{SD}}, \tilde{\mathrm{Z}}_{RD}) = Q\left(\sqrt{\frac{\Phi_0 \sum_{n=1}^{K} \upsilon_{in}^2 \sum_{\tilde{l}=1}^{K_D} \left|\tilde{z}_{\tilde{l},n}^{(SD)}\right|^2}{2KK_0} + \frac{\Phi_1 \sum_{n=1}^{K} \upsilon_{in}^2 \sum_{l=1}^{K_D} \left|\tilde{z}_{l,n}^{(RD)}\right|^2}{2KK_0}}\right). \tag{25}$$

The average PEP for the cooperation mode is:

$$\tilde{E}_{\tilde{\mathrm{Z}}_{SD},\tilde{\mathrm{Z}}_{RD}}\left\{Q\left(\sqrt{\frac{\Phi_0 \sum_{n=1}^{K} \upsilon_{in}^2 \sum_{\tilde{l}=1}^{K_D} \left|\tilde{z}_{\tilde{l},n}^{(SD)}\right|^2}{2KK_0} + \frac{\Phi_1 \sum_{n=1}^{K} \upsilon_{in}^2 \sum_{l=1}^{K_D} \left|\tilde{z}_{l,n}^{(RD)}\right|^2}{2KK_0}}\right)\right\} = \frac{1}{\pi}\int_0^{\frac{\pi}{2}} \left(\frac{4\mu_{SD}^2 z_{SD}(2(z_{SD}+\mathrm{Z}_{SD})\mu_{SD}+g_{PSK}\bar{\kappa}_{SD}/\sin^2(\theta))^{-1}}{\left(2(z_{SD}-\mathrm{Z}_{SD})\mu_{SD}+g_{PSK}\frac{\bar{\kappa}_{SD}}{\sin^2(\theta)}\right)}\right)^{\mu_{SD}} \times \left(\frac{4\mu_{RD}^2 z_{RD}\left(2(z_{RD}+\mathrm{Z}_{RD})\mu_{RD}+g_{PSK}\frac{\bar{\kappa}_{RD}}{\sin^2(\theta)}\right)^{-1}}{\left(2(z_{RD}-\mathrm{Z}_{RD})\mu_{RD}+g_{PSK}\frac{\bar{\kappa}_{RD}}{\sin^2}(\theta)\right)}\right)^{\mu_{RD}} \mathrm{d}\theta\,. \tag{26}$$

After performing some algebraic manipulations, the expression can be represented in terms of a generalized Lauricella hypergeometric function $F_D^{(n)}(.)$ of n variables [24] as:

$$P_{S\to D,R\to D}(\mathrm{S}_0 \to \mathrm{S}_i) = \frac{\nabla_{MRC}(g_{PSK})\Gamma(2\mu_{SD}+2\mu_{RD}+\frac{1}{2})}{2\sqrt{\pi}\Gamma(2\mu_{SD}+2\mu_{RD}+\frac{1}{2})} \times F_D^{(4)}\left[2\mu_{SD}+2\mu_{RD}+\frac{1}{2}; \mu_{SD}, \mu_{SD}, \mu_{RD}; \mu_{RD}; 2\mu_{SD}+2\mu_{RD}+1; \frac{1}{A_1}, \frac{1}{A_2}, \frac{1}{B_1}, \frac{1}{B_2}\right], \tag{27}$$

where

$$\nabla_{MRC}(g_{PSK}) = \left[\frac{4\mu_{SD}^2(z_{SD}^2 - \mathrm{Z}_{SD}^2)}{g^2{}_{PSK}\bar{\kappa}_{SD}^2}\right]^{\mu_{SD}} \times \left[\frac{4\mu_{RD}^2(z^2{}_{RD} - \mathrm{Z}^2{}_{RD})}{g^2{}_{PSK}\bar{\kappa}_{RD}^2}\right]^{\mu_{RD}},$$

$$\begin{Bmatrix} A_1 \\ A_2 \end{Bmatrix} = \frac{\bar{\kappa}_{SD}g_{PSK}}{2\left[z_{SD}\begin{Bmatrix} - \\ + \end{Bmatrix}\mathrm{Z}_{SD}\right]\mu_{SD}} \tag{28}$$

and

$$\begin{Bmatrix} B_1 \\ B_2 \end{Bmatrix} = \frac{\bar{\kappa}_{RD}g_{PSK}}{2\left[z_{RD}\begin{Bmatrix} - \\ + \end{Bmatrix}\mathrm{Z}_{RD}\right]\mu_{RD}}\,. \tag{29}$$

Finally, the average PEP $\bar{P}_e(\mathrm{S}_0 \to \mathrm{S}_i)$ is:

$$\begin{aligned}&\bar{P}_e(\mathrm{S}_0 \to \mathrm{S}_i) = \\ &\bar{P}_{S\to D}(\mathrm{S}_0 \to \mathrm{S}_i) \times \bar{P}_{S\to R} + \\ &\bar{P}_{S\to D,R\to D}(\mathrm{S}_0 \to \mathrm{S}_i) \times (1 - \bar{P}_{S\to R})\,.\end{aligned} \tag{30}$$

At high SNR, $1 - \bar{P}_{S\to R} \approx 1$ and Eq. (30) is:

$$\begin{aligned}&\bar{P}_e(\mathrm{S}_0 \to \mathrm{S}_i) = \\ &\quad \bar{P}_{S\to D}(\mathrm{S}_0 \to \mathrm{S}_i) \times \bar{P}_{S\to R} + \bar{P}_{S\to D,R\to D}(\mathrm{S}_0 \to \mathrm{S}_i)\,.\end{aligned} \tag{31}$$

The union bound of $\bar{P}_e(\mathrm{S}_0 \to \mathrm{S}_i)$ is:

$$\bar{P}_e \le \sum_{i=1}^{|C|} P_e(\mathrm{S}_0 \to \mathrm{S}_i)\,. \tag{32}$$

4.2. Asymptotic PEP Expression

Here, we derive the asymptotic PEP expression which provides significant understandings of the effect of the participating parameters on the end-to-end network performance. The asymptotic PEP is investigated for higher SNR values. For higher SNR values, the approximate MGF for the η–μ fading channel can be expressed as:

$$\begin{aligned}MGF_{\kappa_{\eta-\mu}}\left[\frac{g}{\sin^2(\theta)}\right] &= \left[\frac{4\mu^2 z}{\left(2(z-\mathrm{Z})\mu + \frac{g\bar{\kappa}}{\sin^2(\theta)}\right)\left(2(z+\mathrm{Z})\mu + \frac{g\bar{\kappa}}{\sin^2(\theta)}\right)}\right]^{\mu} \\ &\approx \left(\frac{4\mu^2 z}{g_{PSK}\bar{\kappa}^2}\right)^{\mu} \sin^{4\mu}(\theta)\,.\end{aligned} \tag{33}$$

Based on this, the conditional error probability $\bar{P}_e$ can be approximated as:

$$\bar{P}_e^{ASY} \approx \left(\frac{4\mu_{SD}^2 z_{SD}}{g_{PSK}^2\bar{\kappa}_{SD}^2}\right)^{\mu_{SD}} \sum_{z=0}^{1} \mathrm{A}_{RD}\left(\frac{4\mu_{RD}^2 z_{RD}}{g_{PSK}^2\bar{\kappa}_{RD}^2}\right)^{\mu_{RD}} \times \mathrm{A}_{SR}\left(\frac{4\mu_{SR}^2 z_{SR}}{g_{PSK}^2\bar{\kappa}_{SR}^2}\right)^{\mu_{SR}}, \tag{34}$$

where g_{PSK}, A_{RD} and A_{SR} for the M-ary-phase shift keying (PSK) constellations is:

$$g_{PSK} = \sin^2\left(\frac{\pi}{M}\right), \tag{35}$$

$$\mathrm{A}_{RD} = \frac{1}{\pi}\int_0^{(M-1)\frac{\pi}{M}} \sin^{4(\mu_{SD}+\mu_{RD})}(\theta)\,\mathrm{d}\theta\,, \tag{36}$$

$$\mathrm{A}_{SR} = \frac{1}{\pi}\int_0^{(M-1)\frac{\pi}{M}} \sin^{4\mu_{SR}}(\theta)\,\mathrm{d}\theta\,, \tag{37}$$

Equation (34) can be expressed, in terms of coding gain G_c and DG G_d, as [25, Eq. (13)]:

$$G_d = 2\mu_{SD} + 2\min(\mu_{SR}, \mu_{RD}) \tag{38}$$

$$G_c = \left(\left[\frac{4\mu_{SD}^2 z_{SD}}{g_{PSK}^2 \varpi_0^2 \delta_{SD}^2} \right]^{\mu_{SD}} \sum_{z=0}^{1} \mathrm{A}_{RD} \left[\frac{4\mu_{RD}^2 z_{RD}}{g_{PSK}^2 \varpi_1^2 \delta_{RD}^2} \right]^{\mu_{RD}} \times \mathrm{A}_{SR} \left[\frac{4\mu_{SR}^2 z_{SR}}{g_{PSK}^2 \varpi_0^2 \delta_{SR}^2} \right]^{\mu_{SR}} \right)^{\frac{-1}{G_d}} . \quad (39)$$

The power ratios ϖ_0 and ϖ_1 are expressed as $\varpi_0 = \frac{\Phi_0}{\Phi}$ and $\varpi_1 = \frac{\Phi_1}{\Phi}$, respectively. It can be readily seen that the DO does not depend on the fading parameters, but it affects G_c. Also, it is important to note that for $\mu_{SD} = \mu_{SR} = \mu_{RD} = 0.50$ the value of $G_d = 2$ (Rayleigh fading case), which confirms the results provided in [26].

4.3. Amount of Fading

Amount of fading (AOF) is a parameter that is useful for evaluating the fading severity of a wireless communication system, and it is given in [27, Eq. (1.27)] as:

$$\mathrm{AOF} = \frac{\mathrm{Variance}(\kappa_{MRC})}{\mathrm{E}(\kappa_{MRC})^2} = \frac{\mathrm{E}(\kappa_{MRC}^2) - \mathrm{E}(\kappa_{MRC})^2}{\mathrm{E}(\kappa_{MRC})^2} . \quad (40)$$

The order moment of the κ_{MRC} in the considered set up can be obtained by [27], [28], giving:

$$\mu_n = (-1)^n \left[\frac{d^n}{ds^n} (MGF_{\kappa_{SD}}(s) MGF_{\kappa_{RD}}(s) \right]_{s=0} . \quad (41)$$

Based on this, the first two moments in Eq. (41) are obtained for $n = 1$ and $n = 2$, namely:

$$E(\kappa_{MRC}) = \frac{\partial MGF_{\kappa_{MRC}}(s)}{\partial s} | s = 0 , \quad (42)$$

$$E(\kappa_{MRC}^2) = \frac{\partial^2 MGF_{\kappa_{MRC}}(s)}{\partial^2 s} | s = 0 . \quad (43)$$

In the case of i.i.d. fading links and when the RN decodes successfully, the minimum value of the AOF can be calculated after performing some manipulations, such as:

$$\mathrm{AOF} = \frac{\mu_{SD}(\mu_{SD}+1)\hbar_1^2 - 2\hbar_2\mu_{SD} - 2\hbar_3\mu_{RD}}{(\hbar_1\mu_{SD} + \hbar_4\mu_{RD})^2} + \frac{\mu_{RD}(\mu_{RD}+1)\hbar_4^2 + 2\delta_{RD}\mu_{SD}\hbar_1\hbar_4}{(\hbar_1\mu_{SD} + \hbar_4\mu_{RD})} - 1 , \quad (44)$$

$$\hbar_1 = \frac{\bar{\kappa}_{SD} z_{SD}}{\mu_{SD}(z^2{}_{SD} - \mathrm{Z}^2{}_{SD})} , \quad (45)$$

$$\hbar_2 = \frac{\bar{\kappa}_{SD}^2}{4\mu^2{}_{SD}(z^2{}_{SD} - \mathrm{Z}^2{}_{SD})} , \quad (46)$$

$$\hbar_3 = \frac{\bar{\kappa}_{RD}^2}{4\mu^2{}_{RD}(z^2{}_{RD} - \mathrm{Z}^2{}_{RD})} , \quad (47)$$

$$\hbar_4 = \frac{\bar{\kappa}_{RD} z_{RD}}{\mu_{RD}(z^2{}_{RD} - \mathrm{Z}^2{}_{RD})} . \quad (48)$$

By remembering that the η–μ fading includes Rayleigh distributions as well as Hoyt and Nakagami-m distributions, the fading severity of these distributions can be calculated by the modification described in [29]–[33].

4.4. Analysis of OPA Factors

To obtain OPA, EPA is not the preferable choice. When SR and RD channel gains are different, EPA is not going to improve the system's performance. In this section, we compare the end-to-end system performance for both EPA and OPA schemes considering the total available power constraints over the η–μ fading channel conditions [33]–[38]. The Karush-Kuhn-Tucker (KKT)-based non-linear optimization problem is:

$$\varpi_{opt} = \arg\min_{\varpi} P_{SER} , \quad (49)$$

$$\text{s.t. } \varpi_0 + \varpi_1 = 1 , \quad (50)$$

$$\varpi_0 \geq 0 \ ; \ \varpi_1 \geq 0 , \quad (51)$$

where the power allocation matrix is represented as $\varpi = [\varpi_0, \ \varpi_1]$. A careful investigation of Eq. (49) shows that it is convex in nature, with parameters ϖ_0 and ϖ_1. The Lagrangian of this KKT problem is [38]:

$$P_{SER} + \hat{\lambda}(\varpi_0 + \varpi_1 - 1) - \varepsilon_0\varpi_0 - \Re_1\varpi_1 , \quad (52)$$

where the Lagrangian multiplier is represented as $\hat{\lambda}$ and ε_0 and $\Re_1$ represents the slack variables. Taking the derivative of expression (52) with respect to ϖ_0 and ϖ_0 and combining both equations, we have:

$$\frac{\partial P_{SER}}{\partial \varpi_0} = \frac{\partial P_{SER}}{\partial \varpi_1} . \quad (53)$$

In order to obtain the OPA factors, asymptotic PEP given in Eq. (34) can be expressed in terms of power allocation factors as:

$$P_{SER} \approx \left[\frac{4\mu_{SD}^2 z_{SD} N_0^2}{g_{PSK}^2 \varpi_0^2 \lambda_{jn}^2 \delta_{SD}^2 \Phi^2} \right]^{\mu_{SD}} \sum_{z=0}^{1} \mathrm{A}_{RD} \left[\frac{4\mu_{RD}^2 z_{RD} N_0^2}{g_{PSK}^2 \varpi_1^2 \lambda_{jn}^2 \delta_{RD}^2 \Phi^2} \right]^{\mu_{RD}} \times \mathrm{A}_{SR} \left[\frac{4\mu_{SR}^2 z_{SR} N_0^2}{g_{PSK}^2 \varpi_0^2 \lambda_{jn}^2 \delta_{SR}^2 \Phi^2} \right]^{\mu_{SR}} . \quad (54)$$

Equation (54) can be written in terms of the CO problem as [39]:

$$\min \left[\frac{\psi_1}{\varpi_0^{2(\mu_{SD}+\mu_{SR})}} + \frac{\psi_2}{\varpi_0^{2\mu_{SD}} \varpi_1^{2\mu_{RD}}} \right] \quad \text{s.t. } \varpi_0 + \varpi_1 = 1 , \quad (55)$$

where

$$\psi_1 = A_{SD} A_{SR} \left[\frac{4\mu_{SR}^2 z_{SR} N_0^2}{g_{PSK}^2 \varpi_0^2 \lambda_{jn}^2 \delta_{SR}^2 \Phi^2} \right]^{\mu_{SR}} , \quad (56)$$

$$\psi_2 = A_{RD}\left[\frac{4\mu_{RD}^2 z_{RD} N_0^2}{g_{PSK}^2 \varpi_1^2 \lambda_{jn}^2 \delta_{RD}^2 \Phi^2}\right]^{\mu_{RD}} . \quad (57)$$

Differentiating P_{SER} with respect to ϖ_0 and ϖ_1 as:

$$\frac{\partial P_{SER}}{\partial \varpi_0} = \frac{-2(\mu_{SD}+\mu_{SR})\psi_1}{\varpi_0^{2(\mu_{SD}+\mu_{SR})+1}} - \frac{2\mu_{SD}\psi_2}{\varpi_0^{2\mu_{SD}+1}\varpi_1^{2\mu_{RD}}} , \quad (58)$$

$$\frac{\partial P_{SER}}{\partial \varpi_1} = -\frac{2\mu_{RD}\psi_2}{\varpi_0^{2\mu_{SD}}\varpi_1^{2\mu_{RD}+1}} . \quad (59)$$

Using the relation given in Eq. (53), we get:

$$\frac{(\mu_{SD}+\mu_{SR})\psi_1}{\psi_2} = \frac{\varpi_0^{2\mu_{SR}+1}}{\varpi_1^{2\mu_{RD}}}\left(\frac{\mu_{RD}}{\varpi_1} - \frac{\mu_{SD}}{\varpi_0}\right) . \quad (60)$$

It can be readily seen that the left-hand side of Eq. (60) depends solely on the fading channel's parameters, so this side will always be positive, and it yields to:

$$\varpi_0 \mu_{RD} \geq \varpi_1 \mu_{SD} . \quad (61)$$

By applying the constraint $\varpi_0 + \varpi_1 = 1$, the following conditions are obtained:

$$\frac{\mu_{SD}}{\mu_{SD}+\mu_{RD}}\Phi < \Phi_S < \Phi \quad (62)$$

and

$$0 < \Phi_1 < \frac{\mu_{RD}}{\mu_{SD}+\mu_{RD}}\Phi . \quad (63)$$

For simplicity, $\mu_{SR} = \mu_{RD} = \mu$ and by substituting $Q = \frac{\varpi_0}{\varpi_1}$, Eq. (60) can be expressed as:

$$Q^{2\mu+1} - \frac{\mu_{SD}}{\mu}Q^{2\mu} - (1+\frac{\mu_{SD}}{\mu})\frac{\psi_1}{\psi_2} = 0 . \quad (64)$$

For $2\mu = 1$ the power allocated for the source and relay can be given as:

$$\Phi_0 = \frac{\mu_{SD} + \sqrt{\mu_{SD}^2 + (1+2\mu_{SD})\frac{\psi_1}{\psi_2}}}{1+\mu_{SD}+\sqrt{\mu_{SD}^2+(1+2\mu_{SD})\frac{\psi_1}{\psi_2}}}\Phi \quad (65)$$

and

$$\Phi_1 = \frac{1}{1+\mu_{SD}+\sqrt{\mu_{SD}^2+(1+2\mu_{SD})\frac{\psi_1}{\psi_2}}}\Phi . \quad (66)$$

5. Average OP Analysis of a MIMO-STBC-based S-DF Relaying Network

In this section, we investigate the average OP of a MIMO-STBC-based S-DF relaying network over η–μ fading channel conditions. The channel is in outage when the instantaneous SNR κ_{SR} is lower than the SNR γ_0-threshold.

Let $P_r(\bar{\Phi})$ represent the probability of the event $\bar{\Phi}$ corresponding to the instantaneous SNR $\kappa_{SR}(k)$ of the SR fading link being lower than the SNR outage threshold γ_0, and $P_r(\Phi) = 1 - P_r(\bar{\Phi})$ represent the probability of the complementary event $\bar{\Phi}$, when $\kappa_{SR}(k)$ is larger than γ_0. The per-frame average OP $\bar{P}_{OUT}(\gamma_0)$ at the destination for the selective DF based MIMO-OSTBC cooperative system can be written as:

$$\bar{P}_{OUT}(\gamma_0) = E_{\hat{\kappa}}\left[P_r(\kappa_{SD} \leq \gamma_0)P_r(\bar{\Phi}) + P_r(\kappa_{SD}+\kappa_{RD} \leq \gamma_0)P_r(\Phi)\right] , \quad (67)$$

where $\hat{\kappa} = [\kappa_{SD}, \kappa_{SR}, \text{and } \kappa_{RD}]$ and $P_r(\kappa_{SD} \leq \gamma_0)$ are the probabilities of outage at the destination for the events $\bar{\Phi}$ and Φ, respectively. Since the SR, SD and RD links fade independently, can be simplified as:

$$\bar{P}_{OUT}(\gamma_0) = E_{\kappa_{SD}}\left[P_r(\kappa_{SD} \leq \gamma_0)\right] \times E_{\kappa_{SR}}\left[P_r(\bar{\Phi})\right] + E_{\kappa_{\gamma_{SD}+\gamma_{RD}}}\left[P_r(\kappa_{SD}+\kappa_{RD} \leq \gamma_0)\right] \times \left\{1 - E_{\kappa_{SR}}\left[P_r(\bar{\Phi})\right]\right\} , \quad (68)$$

$$\bar{P}_{OUT}(\gamma_0) = \bar{F}_{\kappa_{SD}}(\gamma_0) \times \bar{F}_{\kappa_{SR}}(\gamma_0) + \bar{F}_{\kappa_{SD}+\kappa_{RD}}(\gamma_0) \times (1 - \bar{F}_{\kappa_{SR}}(\gamma_0)) , \quad (69)$$

where $\bar{F}_{\kappa_{SR}}(\gamma_0)$, $\bar{F}_{\kappa_{SD}}(\gamma_0)$ are provided in Eqs. (72), (74) and $\bar{F}_{\kappa_{SD}+\kappa_{RD}}(\gamma_0)$ is the CDF of the sum of the two independent gamma RVs which can be evaluated in Eq. (75). The instantaneous OP of the SR fading link is:

$$\bar{F}_{\kappa_{SR}}(\bar{\kappa}_{SR}, \gamma_o) = P(\bar{\kappa}_{SR}\|Z_{SR}\|_F^2 < \gamma_o) . \quad (70)$$

The average OP can be evaluated by substituting Eq. (3) in the above expression as:

$$\bar{F}_{\kappa_{SR}}(\bar{\kappa}_{SR}, \gamma_0) = \int_0^{\gamma_0} \frac{2\sqrt{\pi}\mu_{SR}^{\mu_{SR}+\frac{1}{2}} z_{SR}^{\mu_{SR}}}{\Gamma(\mu_{SR}) Z_{SR}^{\mu_{SR}-\frac{1}{2}} \bar{\kappa}_{SR}^{\mu_{SR}+\frac{1}{2}}} \bar{\kappa}_{SR}^{\mu_{SR}-\frac{1}{2}} \times e^{-\frac{2\mu_{SR} z_{SR} \kappa_{SR}}{\bar{\kappa}_{SR}}} \times I_{\mu_{SR}-\frac{1}{2}}\left(\frac{2\mu_{SR} Z_{SR} \kappa_{SR}}{\bar{\kappa}_{SR}}\right) d\kappa_{SR} . \quad (71)$$

OP is the CDF of the received instantaneous SNR, as mentioned earlier and as seen above. Thus, the CDF of η–μ distributed instantaneous SNR, given below, may be used to compute the OP of MIMO-STBC systems over η–μ fading channels.

$$\bar{F}_{\kappa_{SR}}(\bar{\kappa}_{SR}, \gamma_o) = 1 - Y_{\mu_{SR}}\left(\frac{Z_{SR}}{z_{SR}}, \sqrt{\frac{2\mu_{SR} z_{SR} \gamma_0}{\bar{\kappa}_{SR}}}\right) , \quad (72)$$

where

$$Y_\mu(\omega, \phi)$$

is called the Yacoub's integral [17]–[19]. It is defined as:

$$Y_{\mu}(\omega,\phi)=\sqrt{\frac{\pi(1-\omega^2)^{\mu}2^{\frac{3}{2}-\mu}}{\Gamma(\mu)\omega^{\mu-\frac{1}{2}}}}\times\int_{\phi}^{\infty}\mathrm{e}^{-\frac{t^2}{2}}t^{2\mu}I_{\mu-\frac{1}{2}}(t\omega^2)\,\mathrm{d}t\ , \tag{73}$$

where

$$-1<\omega<1$$

and

$$\phi\geq 0\ .$$

Using Yacoub's integral the $\bar{F}_{\kappa_{SD}}(\gamma_0)$ and $\bar{F}_{\kappa_{SD}+\kappa_{RD}}(\gamma_0)$ are:

$$\bar{F}_{\kappa_{SD}}(\bar{\kappa}_{SD},\gamma_o)=1-Y_{\mu_{SD}}\left[\frac{Z_{SD}}{z_{SD}},\sqrt{\frac{2\mu_{SD}z_{SD}\gamma_0}{\bar{\kappa}_{SD}}}\right]\ , \tag{74}$$

$$\bar{F}_{\kappa_{SD}+\kappa_{RD}}(\gamma_0)=$$
$$\left\{1-Y_{\mu_{SD}}\left(\frac{Z_{SD}}{z_{SD}},\sqrt{\frac{2\mu_{SD}z_{SD}\gamma_0}{\bar{\kappa}_{SD}}}\right)\right\}\times$$
$$\left\{1-Y_{\mu_{RD}}\left(\frac{Z_{RD}}{z_{RD}},\sqrt{\frac{2\mu_{RD}z_{RD}\gamma_0}{\bar{\kappa}_{RD}}}\right)\right\}\ . \tag{75}$$

6. Simulation Results

In this section, the end-to-end performance and OPA of MIMO-STBC-based S-DF relaying networks is investigated over the η–μ fading channel conditions. Over i.i.d. and i.n.i.d. channels, exact and asymptotic formulas for the end-to-end PEP, assuming MPSK modulated signals, is obtained. The analytic expressions obtained are then employed to gain insight into the various fading parameters in the η–μ fading channel scenarios, as well as to assess their impact on end-to-end PEP and OP performance. To that aim, performance curves depicting average PEP versus SNR in dB for M-ary QAM modulation symbols are shown,

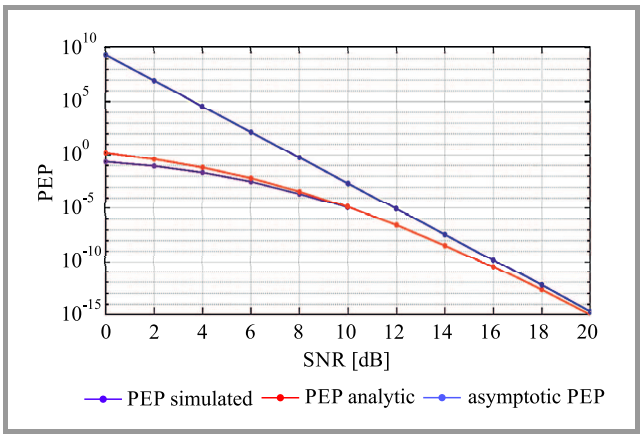

Fig. 2. PEP versus SNR performance, in dB, for 4-PSK symbols over i.i.d. η–μ fading channel conditions considering $\mu_{SD}=\mu_{SR}=\mu_{RD}=0.50$, $\eta_{SD}=\eta_{SR}=\eta_{RD}=0.50$, and average channel gains of the SD, SR and RD links are: $\delta^2_{SD}=\delta^2_{RD}=\delta^2_{SR}=0$ dB.

with the overall transmit power being assigned equally or optimally to the SN and RN using the power strategy developed in Section 3. Figure 2 demonstrates the average PEP performance as a function of SNR for MIMO STBC-based S-DF cooperative systems utilizing EPA factors, i.e. $\Phi_0=\Phi_1=\Phi/2$, for symmetric and balanced η–μ fading channels considering the 4-PSK constellations.
Furthermore, the η–μ fading parameters are: $\mu_{SD}=\mu_{SR}=\mu_{RD}=0.50$, $\eta_{SD}=\eta_{SR}=\eta_{RD}=0.50$, and the average channel gains of the SD, SR and RD links are: $\delta^2_{SD}=\delta^2_{RD}=\delta^2_{SR}=0$ dB. Because of the good agreement between the exact outcomes of PEP and OP expressions and the results of corresponding computer simulations, their validity has been shown. A complete diversity order of 2 can be attained, with the exact results being firmly limited by asymptotic curves in the spectrum from low SNR values to high SNR regimes. The DG (exact), DG (asymp.) and DG Eq. (39) – are given as 1.95, 2 and 2, respectively, where it is assumed that $\Phi_0=\Phi$. MIMO-STBC-based S-DF systems outperform direct transmission (SD transmission) scenarios by roughly 15 dB and 21.5 dB, respectively, at 10^4 target PEP.

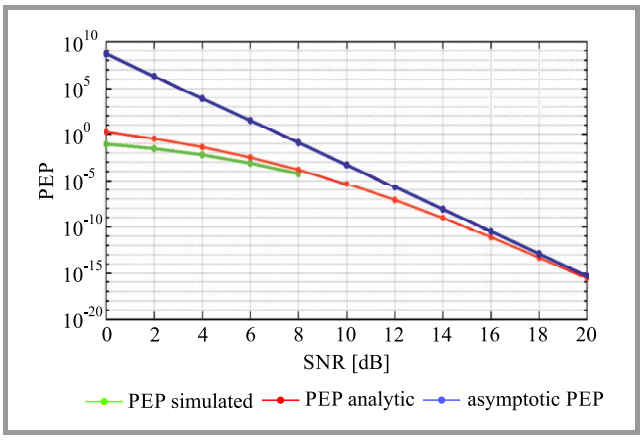

Fig. 3. PEP versus SNR performance, in dB, for 4-PSK symbols over i.i.d. η–μ fading channel conditions considering with $\mu_{SD}=\mu_{SR}=\mu_{RD}=1.50$ and $\eta_{SD}=\eta_{SR}=\eta_{RD}=1$ as well as balanced links, i.e. average channel gains of the SD, SR and RD links are: $\delta^2_{SD}=\delta^2_{RD}=\delta^2_{SR}=0$ dB.

In the same context, Fig. 3 shows the average PEP performance as a function of SNR for 16-QAM modulation symbols for a single relay MIMO STBC-based S-DF network considering the EPS factors over symmetric η–μ fading channels with $\mu_{SD}=\mu_{SR}=\mu_{RD}=1.50$ and $\eta_{SD}=\eta_{SR}=\eta_{RD}=1$ as well as balanced links, i.e. average channel gains of the SD, SR and RD links are: $\delta^2_{SD}=\delta^2_{RD}=\delta^2_{SR}=0$ dB. It is further demonstrated that the exact analytical PEP curves closely match the simulation curves for medium and high SNR values, and that the asymptotic curves tend to be nearly the exact copies of those for PEP lower than 10^4. As a result, in actual S-DF relaying system designs with high SNR, the provided asymptotic formulas might provide important system performance insights.

In Fig. 4, a MIMO STBC S-DF single relay network is considered with QPSK symbols and EPA factors taken into account. The simulation parameters are given as: $\mu_{SD} = \mu_{SR} = \mu_{RD} = \{1,2,3\}$ and the average channel gains of the SD, SR and RD links are: $\delta^2_{SD} = \delta^2_{RD} = \delta^2_{SR} = 0$ dB. It is evident that the Hoyt distribution is equal to the η–μ fading distribution when $\mu_{SD} = \mu_{SR} = \mu_{RD} = 0.50$. We can see the impact of the scattered-wave power ratio on the average PEP of the proposed MIMO-STBCD-based S-DF network by changing the value of η. This proves that PEP is inversely proportional to η, since when η increases from 1 to 3 for all values of μ, an average gain of 2 dB is observed for the target average PEP of 10^{-5}. Furthermore, when μ increases from 1 to 3 and μ increases from 2 to 3, average improvements of 3.89 dB and 1.65 dB are attained.

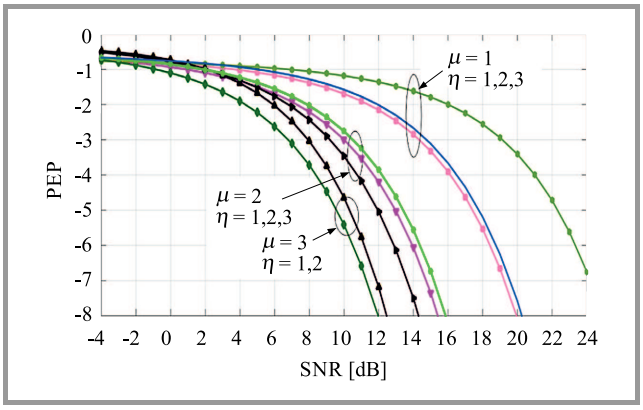

Fig. 4. PEP vs. SNR, in dB, with $\mu_{SD} = \mu_{SR} = \mu_{RD} = \{1,2,3\}$, η increases from 1 to 3 QPSK and EPA factors.

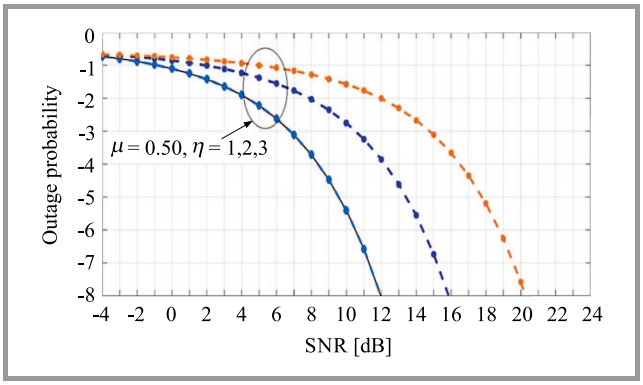

Fig. 5. SER vs. SNR with $\mu_{SD} = \mu_{SR} = \mu_{RD} = \mu = \{0.50\}$ with η increasing from 1 to 3 for 4-PSK considering the EPA factors.

In the similar manner, Fig. 5 demonstrates the average OP performance for 4-PSK modulation symbols under the independent and non-identically distributed η–μ fading channels, for single relays with EPA factors. The simulation parameters are: $\delta^2_{SD} = \delta^2_{SR} = 1, \delta^2_{RD} = 10$ dB, $\mu_{SD} = \mu_{SR} = \mu_{RD} = \mu = \{0.50\}$ dB, with η increasing from 1 to 3. When the values of η change from 1 to 3 for δ^2_{RD} = 10 dB, for the considered values of $\mu_{SD} = \mu_{SR} = \mu_{RD} = \mu = \{0.50\}$, the system's performance improves significantly. At OP of nearly 1.25 dB and 1.75 dB, gains are achieved when the values of η_{SR} and η_{RD} change from 1 to 3 for the considered values of η.

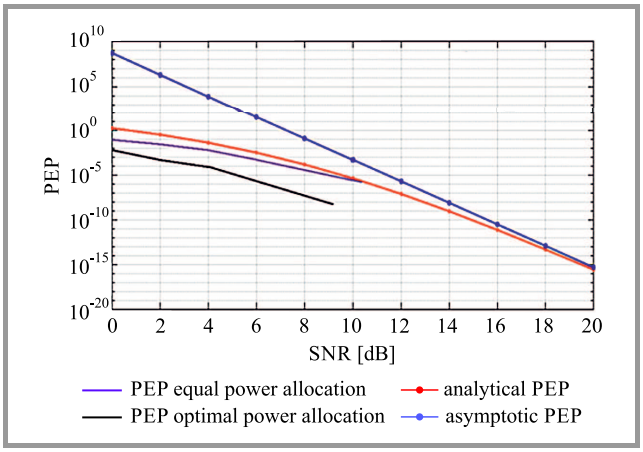

Fig. 6. PEP vs. SNR performance, in dB, for quadrature PSK symbols over i.i.d. fading channel conditions for OPA factors.

Figure 6 shows PEP performance of the proposed OPA scheme and assumes a greater channel variance from the RNs to the DN, with a constant scattered-wave power ratio for single relays and QPSK constellations. The simulation parameters are: $\mu_{SD} = \mu_{SR} = \mu_{RD} = \mu = 0.50$, $\delta^2_{SD} = \delta^2_{SR} =$ 0 dB, $\delta^2_{RD} = 100$ dB and $\eta = 0.50$. The OPA factors are $\varpi_0 = 0.90$ and $\varpi_0 + \varpi_1$ = 1-0.98. It has been assumed that when μ is small, such as $\mu = 0.50$, the proposed OPA scheme creates a cooperation mechanism offering minor benefits which, however, grow as μ increases. Indicatively, the optimal method surpasses the EPA scenario by at least 1.5 dB when $\mu = 0.50$ for a PEP of 10^{-4}.

7. Conclusion

In this paper, we have investigated end-to-end PEP and average OP performance of MIMO-STBC-based S-DF relaying networks under η–μ fading channel conditions. The exact and asymptotic end-to-end PEP expression, assuming modulated M-ary-PSK and M-ary-QAM complex modulated symbols, have been produced on i.i.d. fading links. The analytical expressions acquired were then used to obtain insights into different fading factors and their effect on end-to-end system performance under non-homogeneous fading channel conditions. The data given were then used in the development of an asymptotically optimal power distribution system, within a total sum power limit, which showed that the standard EPA technique was substantially outperformed. The OPA system is also demonstrated to be virtually separate from the power ratio parameter dispersed waves from SN to DN, depending upon the number of multipath clusters and on the chosen modulating system. The curves demonstrate that for moderate and high SNR regimes, the asymptotic and exact expressions are closely

matching. PEP performance is noticeably increased as and increase as with a PEP of plots show that the OPA schemes outperform the EPA schemes.

References

[1] M. K. Beuria, R. Shankar, and S. S. Singh, "Analysis of the energy harvesting non-orthogonal multiple access technique for defense applications over Rayleigh fading channel conditions", *The J. of Defense Model. and Simulation*, 2021 (DOI: 10.1177/15485129211021168).

[2] S. N. Swain, R. Thakur, and S. R. M. Chebiyyam, "Coverage and rate analysis for facilitating machine-to-machine communication in LTE-A networks using device-to-device communication", *IEEE Trans. on Mob. Comput.*, vol. 16, no. 11, pp. 3014–3027, 2017 (DOI: 10.1109/TMC.2017.2684162).

[3] S. Pandya, M. A. Wakchaure, R. Shankar, and J. R. Annam, "Analysis of NOMA-OFDM 5G wireless system using deep neural network", *The J. of Defense Model. and Simul.*, 2021 (DOI: 10.1177/1548512921999108).

[4] R. Shankar, "Examination of a non-orthogonal multiple access scheme for next generation wireless networks", *The J. of Defense Model. and Simul.*, 2020 (DOI: 10.1177/1548512920951277).

[5] R. Shankar, K. N. Pandey, A. Kumari, V. Sachan, and R. K. Mishra, "C(0) protocol based cooperative wireless communication over Nakagami-m fading channels: PEP and SER analysis at optimal power", in *Proc. IEEE 7th Ann. Comput. and Commun. Worksh. and Conf. CCWC 2017*, Las Vegas, NV, USA, 2017 (DOI: 10.1109/CCWC.2017.7868399).

[6] N. Varshney, A. V. Krishna, and A. K. Jagannatham, "Selective DF protocol for MIMO STBC based single/multiple relay cooperative communication: end-to-end performance and optimal power allocation", *IEEE Trans. on Commun.*, vol. 63, no. 7, pp. 2458–2474, 2015 (DOI: 10.1109/TCOMM.2015.2436912).

[7] N. Varshney, A. K. Jagannatham, and P. K. Varshney, "Cognitive MIMO-RF/FSO cooperative relay communication with mobile nodes and imperfect channel state information", *IEEE Trans. on Cognitive Commun. and Network.*, vol. 4, no. 3, pp. 544–555, 2018 (DOI: 10.1109/TCCN.2018.2844827).

[8] K. Eltira, N. Jibreel, A. Younis, and R. Mesleh, "Capacity analysis of cooperative amplify and forward multiple-input multiple-output systems", *Trans. on Emerg. Telecommun. Technol.*, vol. 32, no. 10 (DOI: 10.1002/ett.4290).

[9] H. K. Boddapati, R. B. Manav, and P. Shankar, "Performance of cooperative multi-hop cognitive radio networks with selective decode-and-forward relays", *IET Commun.*, vol. 12, no. 20, pp. 2538–2545, 2018 (DOI: 10.1049/iet-com.2018.5328).

[10] A. Z. Afify, A. Shawky, and N. Mazen, "A new inverse Weibull distribution: properties, classical and Bayesian estimation with applications", *Kuwait J. of Sci.*, vol. 48, no. 3, 2021 (DOI: 10.48129/kjs.v48i3.9896).

[11] E. M. Almetwally *et al.*, "Marshall-Olkin alpha power Weibull distribution: Different methods of estimation based on type-I and type-II censoring", *Complexity*, vol. 2021, article ID 5533799, 2021 (DOI: 10.1155/2021/5533799).

[12] R. Shankar, I. Kumar, A. Kumari, K. N. Pandey, and R. K. Mishra, "Pairwise error probability analysis and optimal power allocation for selective decode-forward protocol over Nakagami-m fading channels", in *Proc. Int. Conf. on Algor., Methodol., Models and Appl. in Emerg. Technol. ICAMMAET 2017*, Chennai, India, 2017 (DOI: 10.1109/ICAMMAET.2017.8186700).

[13] R. Shankar and R. K. Mishra, "An investigation of S-DF cooperative communication protocol over keyhole fading channel", *Phys. Commun.*, vol. 29, pp. 120–140, 2018 (DOI: 10.1016/j.phycom.2018.04.027).

[14] R. Shankar and R. K. Mishra, "EP and OP examination of relaying network over time-selective fading channel", *SN Appl. Sci.*, vol. 2, article ID: 1329, 2020 (DOI: 10.1007/s42452-020-3077-5).

[15] R. Shankar and R. K. Mishra, "S-DF cooperative communication system over time selective fading channel", *J. of Inform. Sci. and Engin.*, vol. 35, no. 6, pp. 1223–1248, 2019 (DOI: 10.6688/JISE.201911_35(6).0004).

[16] R. Shankar and R. K. Mishra, "Outage probability analysis of selective-decode and forward cooperative wireless network over time varying fading channels with node mobility and imperfect CSI condition", in *Proc. TENCON 2018 — 2018 IEEE Region 10 Conf.*, Jeju, South Korea, 2018, pp. 0508–0513 (DOI: 10.1109/TENCON.2018.8650275).

[17] C. B. Issaid, M.-S. Alouini, and R. Tempone, "On the fast and precise evaluation of the outage probability of diversity receivers over η–μ, κ–μ, and η–μ fading channels", *IEEE Trans. Wirel. Commun.*, vol. 17, no. 2, pp. 1255–1268, 2018 (DOI: 10.1109/TENCON.2018.8650275).

[18] O. S. Badarneh and F. S. Almehmadi, "Performance analysis of L-branch maximal ratio combining over generalized η–μ fading channels with imperfect channel estimation", *IET Commun.*, vol. 10, no. 10, pp. 1175–1182, 2016 (DOI: 10.1049/iet-com.2015.1015).

[19] F. S. Almehmadi and O. S. Badarneh, "Performance analysis of outage probability and error rate of square M-QAM in mobile wireless communication systems over generalized α–μ fading channels with non-Gaussian noise", *China Commun.*, vol. 15, no. 1, pp. 62–71, 2018 (DOI: 10.1109/CC.2018.8290806).

[20] H. Yu, G. Wei, F. Ji, and X. Zhang, "On the error probability of cross-QAM with MRC reception over generalized η–μ fading channels", *IEEE Trans. on Veh. Technol.*, vol. 60, no. 6, pp. 2631–2643, 2011, (DOI: 10.1109/TVT.2011.2154347).

[21] M. Bilim, "QAM signaling over κ–μ shadowed fading channels", *Phys. Commun.*, vol. 34, pp. 261–271, 2019 (DOI: 10.1016/j.phycom.2019.04.005).

[22] M. Bilim and N. Kapucu, "On the analysis of achievable rate for NOMA networks with cooperative users over κ–μ shadowed fading channels", *Int. J. Commun. Syst.*, vol. 32, no. 12, 2019 (DOI: 10.1002/dac.4001).

[23] S. Kumar and S. Kalyani, "Outage probability and rate for κ–μ shadowed fading in interference limited scenario", *IEEE Trans. Wirel. Commun.*, vol. 16, no. 12, pp. 8289–8304, 2017 (DOI: 10.1109/TWC.2017.2760822).

[24] O. S. Badarneh and R. Mesleh, "A comprehensive framework for quadrature spatial modulation in generalized fading scenarios", *IEEE Trans. Commun.*, vol. 64, no. 7, pp. 2961–2970, 2016 (DOI: 10.1109/TCOMM.2016.2571285).

[25] N. Bhargav, S. L. Cotton, and E. David Simmons, "Secrecy capacity analysis over κ–μ fading channels: theory and applications", *IEEE Trans. Commun.*, vol. 64, no. 7, pp. 3011–3024, 2016 (DOI: 10.1109/TCOMM.2016.2565580).

[26] J. M. Moualeu and W. Hamouda, "On the secrecy performance analysis of SIMO systems over κ–μ fading channels", *IEEE Commun. Lett.*, vol. 21, no. 11, pp. 2544–2547, 2017 (DOI: 10.1109/LCOMM.2017.2741458).

[27] J. M. Moualeu *et al.*, "Physical-layer security of SIMO communications systems over multipath fading conditions", *IEEE Trans. on Sustain. Comput.*, vol. 6, no. 1, pp. 105–118, 2019 (DOI: 10.1109/TSUSC.2019.2915547).

[28] H. Lei, I. S. Ansari, G. Pan, B. Alomair, and M.-S. Alouini, "Secrecy capacity analysis over α–μ fading channels", *IEEE Commun. Lett.*, vol. 21, no. 6, pp. 1445–1448, 2017 (DOI: 10.1109/LCOMM.2017.2669976).

[29] J. M. Moualeu, D. B. da Costa, W. Hamouda, U. S. Dias, and R. A. A. de Souza, "Physical layer security over α–κ–μ and α–η–μ fading channels", *IEEE Trans. on Veh. Technol.*, vol. 68, no. 1, pp. 1025–1029, 2019 (DOI: 10.1109/TVT.2018.2884832).

[30] J. Yang, L. Chen, X. Lei, K. P. Peppas, and T. Q. Duong," Dual-hop cognitive amplify-and-forward relaying networks over η–μ fading channels", *IEEE Trans. on Veh. Technol.*, vol. 65, no. 8, pp. 6290–6300, 2015 (DOI: 10.1109/TVT.2015.2480968).

[31] S. H. Alvi, S. Wyne, and D. B. da Costa, "Performance analysis of dual-hop AF relaying over α–μ fading channels", *AEU-Int. J. of Electron. and Commun.*, vol. 108, pp. 221–225, 2019 (DOI: 10.1016/j.aeue.2019.06.013).

[32] J. M. Moualeu, T. M. N. Ngatched, and D. B. da Costa, "Sequential relay selection in D2D-enabled cellular networks with outdated CSI over mixed fading channels", *IEEE Wirel. Commun. Lett.*, vol. 8, no. 1, pp. 245–248, 2019 (DOI: 10.1109/LWC.2018.2868645).

[33] S. Kumar *et al.*, "Energy detection based spectrum sensing for gamma shadowed α–η–μ and α–κ–μ fading channels", *AEU-Int. J. of Electron. and Commun.*, vol. 93, pp. 26–31, 2018 (DOI: 10.1016/j.aeue.2018.05.031).

[34] T. F. Hailat, H. B. Salameh, and T. Aldalgamouni. "Performance study of multi-hop communication systems with decode-and-forward relays over α–μ fading channels", *IET Commun.*, vol. 11, no. 10, pp. 1641–1648, 2017 (DOI: 10.1049/iet-com.2016.1220).

[35] A. Hussain, A. K. Lee, S.-H. Kim, S.-H. Chang, and D. I. Kim, "Performance analysis of dual-hop variable-gain relaying with beamforming over κ–μ fading channels", *IET Commun.*, vol. 11, no. 10, pp. 1587–1593, 2017 (DOI: 10.1049/iet-com.2016.1102).

[36] R. Shankar, L. Bhardwaj, and R. K. Mishra, "Analysis of selective-decode and forward relaying protocol over κ–μ fading channel distribution", *J. of Telecommun. and Inform. Technol.*, no. 1, pp. 21–30, 2020 (DOI: 10.26636/jtit.2020.135919).

[37] Y. J. Chun *et al.*, "A Comprehensive analysis of 5G heterogeneous cellular systems operating over κ–μ shadowed fading channels", *IEEE Trans. on Wirel. Commun.*, vol. 16, no. 11, pp. 6995–7010, 2017 (DOI: 10.1109/TWC.2017.2734080).

[38] K. P. Peppas, G. C. Alexandropoulos, and P. T. Mathiopoulos, "Performance analysis of dual-hop AF relaying systems over mixed η–μ and κ–μ fading channels", *IEEE Trans. on Veh. Technol.*, vol. 62, no. 7, pp. 3149–3163, 2013 (DOI: 10.1109/TVT.2013.2251026).

[39] D. Pant, P. S. Chauhan, S. K. Soni, and S. Naithani, "Channel capacity analysis of wireless system under ORA scheme over κ–μ inverse gamma and η–μ/ inverse gamma composite fading models", in *Proc. of Int. Conf. on Elec. and Electron. Engin. ICE3 2020*, Gorakhpur, India, 2020, pp. 425–430 (DOI: 10.1109/ICE348803.2020.9122938).

[40] S. K. Yoo, S. L. Cotton, P. C. Sofotasios, S. Muhaidat, and G. K. Karagiannidis, "Effective capacity analysis over generalized composite fading channels", *IEEE Access*, vol. 8, pp. 123756–123764, 2020 (DOI: 10.1109/ACCESS.2020.3003207).

[41] C. Ben Issaid, M. Alouini, and R. Tempone, "On the fast and precise evaluation of the outage probability of diversity receivers over α–μ, and η–μ fading channels", *IEEE Trans. on Wirel. Commun.*, vol. 17, no. 2, pp. 1255–1268, 2018 (DOI: 10.1109/TWC.2017.2777465).

[42] M. Bilim, "Uplink communication with AWGN over non-homogeneous fading channels", *Phys. Commun.*, vol. 39, no. C, 2020 (DOI: 10.1016/j.phycom.2020.101047).

[43] P. Kumar and K. Dhaka, "Performance analysis of a decode-and-forward relay system in κ-μ and η-μ fading channels", *IEEE Trans. on Veh. Technol.*, vol. 65, no. 4, pp. 2768–2775, 2016 (DOI: 10.1109/TVT.2015.2418211).

[44] K. Papazafeiropoulos and S. A. Kotsopoulos, "Second-order statistics for the envelope of α–*kappa*–μ fading channels", *IEEE Commun. Lett.*, vol. 14, no. 4, pp. 291–293, 2010 (DOI: 10.1109/LCOMM.2010.04.092265).

[45] B. Samudhyatha, S. Gurugopinath, and K. Saraswathi, "Maximum eigenvalue-based spectrum sensing over α–κ–μ and α–η–μ fading channels", in *Proc. of IEEE 28th Ann. Int. Symp. on Pers., Indoor, and Mob. Radio Commun. PIMRC 2017*, Montreal, QC, Canada, 2017 (DOI: 10.1109/PIMRC.2017.8292575).

Ravi Shankar received his B.E. in Electronics and Communication Engineering from Jiwaji University, Gwalior, India, in 2006. He received his M.Tech. degree in Electronics and Communication Engineering from GGSIPU, New Delhi, India, in 2012. He received a Ph.D. in Wireless Communication from the National Institute of Technology Patna, Patna, India, in 2019. From 2013 to 2014 he was an Assistant Professor at MRCE Faridabad, where he was engaged in researching wireless communication networks. He is presently an assistant professor at MITS Madanapalle, Madanapalle, India. His current research interests cover cooperative communication, D2D communication, IoT/M2M networks and networks protocols. He is a student member of IEEE.

https://orcid.org/0000-0001-7532-3275
E-mail: ravishankar.nitp@gmail.com
Department of Electronics and Communication Engineering
Madanapalle Institute of Technology and Science
Andhra Pradesh
517325, India

V. V. Raghava Raman holds a Ph.D. in Computer Science and Engineering. He has over two decades of experience in teaching at national and international levels. He has guided research scholars in the area of the Internet of Things. His areas of interest cover data warehousing, data mining, programming languages, AI and IoT.
Department of Computer Science
Aurora's Degree and PG College
Chikkadapally
Hyderabad, India

Kantilal P. Rane is presently working as a Professor at Department of Electronics and Communication, K L University, Hyderabad. He completed his Ph.D. in 2013 from North Maharashtra University, Jalgaon. His areas of research includes antennas, wave propagation, electromagnetic field theory, VLSI and embedded system design, as well as networking.
E-mail: kantiprane@rediffmail.com
Department of Electronics and Communication
K L University
Hyderabad, India

Sarojini B. K. received her Ph.D. in Computer and Information Engineering from Vishweshwaraya Technological University (VTU) Belagavi, Karnataka. She completed her M.Tech. at the ECE Department of the Indian Institute of Technology Kharagpur and B.E. in Electronics and Communication Engineering from Mysore University. Currently, she is a professor at the Department of Electronics and Communication Engineering, Basaveshwar Engineering College, Bagalkot, Karnataka. Her research interests include signal processing, machine learning and communication.

E-mail: srjnsarojini@gmail.com
Department of ECE
Basaveshwar Engineering College
Bagalkot-587103, Karnataka, India

Rahul Neware received his B.E. in Information Technology from RTM Nagpur University India, in 2015, and M.Tech. in Computer Science and Engineering from G. H. Raisoni College of Engineering, Nagpur, India, in 2018. He is currently pursuing a Ph.D. in Computing from Western Norway University of Applied Sciences, Bergen campus, Norway. His interests focus on cybersecurity, cloud and fog computing, advanced image processing and remote sensing.

E-mail: rane@hvl.no
Høgskulen på Vestlandet
Bergen, Norway